Polarized electron scattering from polarized deuterium at BLAST

K. A. Dow

MIT-Bates Linear Accelerator Center and Laboratory for Nuclear Science, Massachusetts Institute of Technology, Cambridge, MA 02139

for the BLAST Collaboration

The Bates Large Acceptance Spectrometer Toroid (BLAST) was built to study the spin-dependent electromagnetic interaction in few-nucleon systems. The experiments use the longitudinally polarized electron beam in the MIT-Bates South Hall Ring, a polarized atomic beam source with the target cell internal to the storage ring, and the symmetric large acceptance BLAST detector. Preliminary results from the vector and tensor polarized deuterium target are presented, including measurements of quasielastic electron scattering, G_E^n, and T_{20}.

PACS: ....
Key words: ....

1 Introduction

The deuteron is the simplest system in which to study the nucleon-nucleon interaction; it is also useful for studying the neutron, in the absence of a free neutron target. The use of a polarized electron beam and a polarized target allows access to smaller form factors, such as G_E^n, through asymmetry measurements.

For polarized electron scattering from a polarized target, the cross section can be written as [1]:

$$S(h, P_z, P_{zz}) = S_0(1 + P_z A_d^V + P_{zz} A_d^T + h(A_e + P_z A_{ed}^V + P_{zz} A_{ed}^T),$$

where h is the electron helicity, P_z is the target vector polarization, P_{zz} is the target tensor polarization, and S_0 is the unpolarized cross section. In the Born approximation, $A_e = A_d^V = A_{ed}^T = 0$. In the absence of the L=2 moment for the deuteron, $A_d^T = 0$. The A_{ed}^V term is also sensitive to the quadrupole moment and effects beyond PWIA, such as meson exchange currents, isobar currents, and relativistic corrections. In Plane-wave Impulse Approximation:

$$A_{ed}^V = \frac{a G_M^{N2} cos\theta^* + b G_E^N G_M^N sin\theta^* cos\phi^*}{c G_E^{N2} + G_M^{N2}},$$

where N represents the detected nucleon (proton or neutron), a,b and c are kinematic factors, and θ^* and ϕ^* describe the direction of the target spin with respect to the momentum transfer. Choosing $\theta^* = \pi/2$ maximizes the sensitivity of the asymmetry to the ratio of electric to magnetic form factors. Thus, a measurement of (e,e′n) with a polarized electron beam and a vector-polarized deuterium target can be used to extract G_E^n.

For the quasielastic reactions, some kinematics definitions of missing energy, momentum and mass will be useful:

$$E_m = m_D + \omega - p_x$$
$$\vec{p}_m = \vec{q} - \vec{p}_x$$
$$m_m = \sqrt{E_m^2 - p_m^2},$$

where m_D is the mass of the deuteron, ω is the energy loss of the electron, $\vec{q}$ is the momentum transfer, and $\vec{p}_x$ is the momentum of the detected nucleon.

The general form for the cross section for elastic electron scattering from deuterium is, using the same terminology as in quasi-elastic scattering:

$$S(h, P_z, P_{zz} = S_0(1 + P_{zz}\Gamma + hP_z\Delta)$$
$$S_0 \propto (A(Q^2) + B(Q^2) tan^2 \frac{\theta_e}{2})$$
$$A(Q^2) = G_C^2(Q^2) + \frac{8}{9}\eta^2 G_Q^2(Q^2) + \frac{2}{3}\eta G_M^2(Q^2)$$
$$B(Q^2) = \frac{4}{3}\eta(1+\eta)G_M^2(Q^2)$$
$$\eta = \frac{Q^2}{4m_d^2},$$

where G_C, G_Q and G_M are the charge, quadrupole and magnetic form factors of the deuteron. With an unpolarized beam and target, a Rosenbluth separation will extract the magnetic form factor and a combination of the charge and quadrupole form factors. However, another measurement is needed to separate all three form factors. This can be done with a tensor-polarized target and an unpolarized electron beam by forming an asymmetry using two target states. The asymmetry depends on P_{zz} and Γ, where

$$\Gamma = \frac{3cos^2\theta_d^* - 1}{2} T_{20} - \sqrt{\frac{3}{2}} \sin 2\theta_d^* cos\phi_d^2 T_{21} + \sqrt{\frac{3}{2}} sin^2\theta_d^* cos\phi_d^* T_{22}$$
$$T_{20} = \frac{-1}{\sqrt{2}S}(\frac{8}{3}\eta G_C G_Q + \frac{8}{9}\eta^2 G_Q^2 + \frac{1}{3}\eta[1 + 2(1+\eta)\tan^2\frac{\theta_e}{2}]G_M^2).$$

T_{21} is proportional to $G_M G_Q$, and can be extracted from the measured asymmetry using two different target spin orientations, or taken from parametrizations of world data. T_{22} is related to G_M^2.

The combination of cross section measurements at two angles and the asymmetry measurement allow one to extract all three form factors from the experimental data.

...

2 The BLAST Experiment

The BLAST experiment made use of a longitudinally polarized 850 MeV cw electron beam in the South Hall Ring at the MIT-Bates Linear Accelerator Center. A Siberian Snake in the ring kept the beam polarization longitudinal at the target, by rotating the electron spin such that the precession in the second half of the ring cancelled the precession in the first half. Currents of up to 225 mA were stacked in the ring, with a beam lifetime of approximately 25-30 minutes with gas in the BLAST target. Slow controls for the accelerator, ring, target and detector used the EPICS control system.

A Compton Polarimeter upstream of the BLAST internal target was used to measure the beam position. Circularly polarized light from a 5 W cw laser at 532 nm was normally incident on the electron beam. The laser helicity was reversed regularly with a Pockels cell, and a chopper wheel was used to block the laser beam for background measurements. Backscattered photons were detected with a CsI crystal to measure the backscatter rate as a function of photon energy. The cross section for backscattered photons depends on the photon energy, as well as the electron and laser helicities. Thus, forming and fitting a photon rate asymmetry as a function of energy allowed the extraction of the electron polarization. The beam polarization was typically 65%, with a systematic uncertainty of less than 3%.

The open-ended cylindrical target cell was 60 cm long, with a diameter of 15 mm. This geometry, together with an upstream collimator, means there was very little background from the cell walls. Isotopically pure polarized deuterium or hydrogen was supplied to the target with an atomic beam source (ABS). The ABS was originally used for experiments at NIKHEF, then extensively modified to work in the BLAST magnetic field of 0.2 T. A deuterium target thickness of 6x10^{13} atoms/cm^2 was achieved. Magnets and RF transitions in the ABS were set to populate the desired spin states of deuterium. We ran a combination of vector and tensor states, with typical polarizations of 70-80% for vector deuterium and 55-67% for tensor deuterium. The target spin angle could be set at an arbitrary angle in the horizontal plane using two sets of holding field coils. We chose to run with the target angle oriented at 32 or 47° in the left sector, and the neutron detectors concentrated in the right sector. This arrangement maximized the experimental sensitivity to G_E^n, as the asymmetry is most sensitive to G_E^n when the target spin is perpendicular to the momentum transfer vector.

The BLAST spectrometer (see Fig. 1) consisted of eight normal-conducting copper coils in a symmetric arrangement about the beam line. This arrangement provided for no field on the beam centerline, and very small field gradients in the internal target region, essential for maintenance of polarization in a polarized ^3He target. The coils ran at 6731 A, providing a toroidal field of up to 3.8 kG. The detectors were arranged symmetrically in the two midplane sectors, with the exception of the neutron detectors, which were concentrated in the beam right sector as mentioned above.

The detectors consisted of drift chambers, scintillators, and Cerenkov and neutron detectors, covering scattering angles of 20 to 80 degrees, and out-of-plane

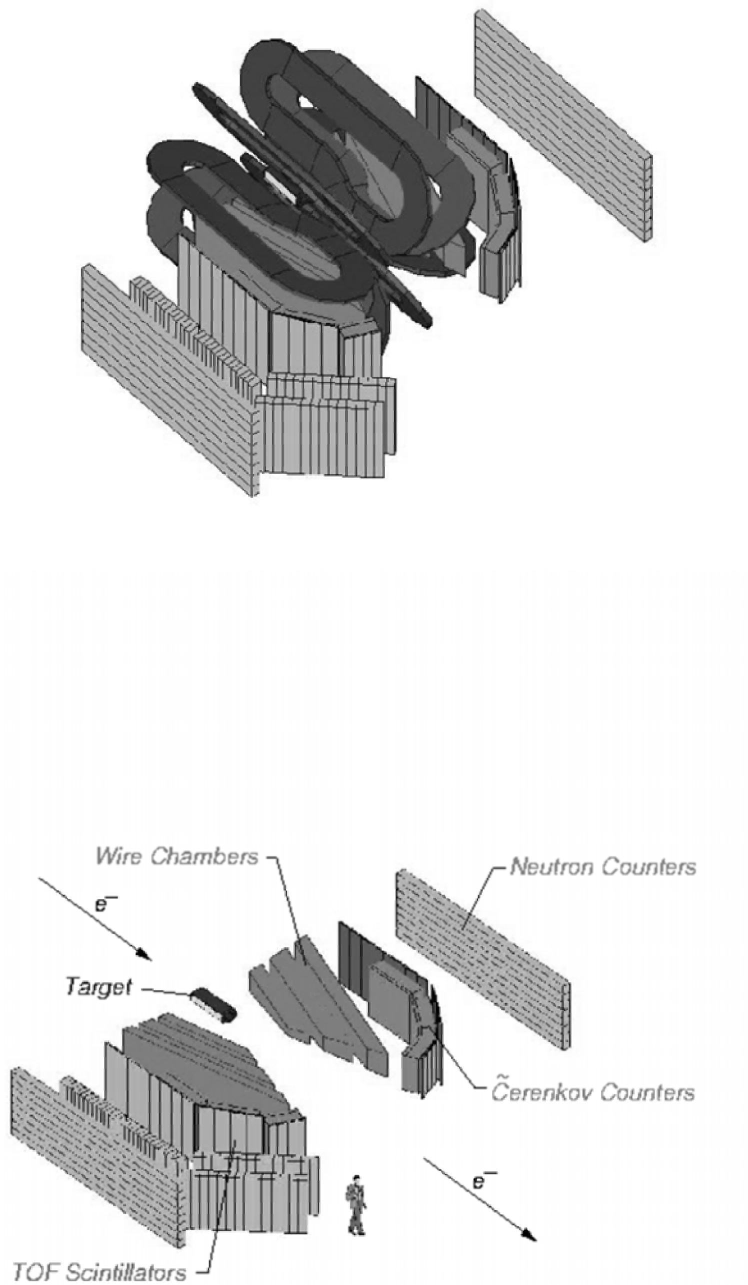

Fig. 1. A view of the BLAST spectrometer, with and without the coils.

angles of +/- 15°. The drift chambers were built of 3 chambers in each sector, with 2 superlayers per chamber (inclined at +/- 5° stereo angle), and 3 layers per superlayer. This arrangement nominally gives 18 wire hits per track, sufficient for reconstruction of the particle momentum, scattering angle and out-of-plane angle. There were 20 time-of-flight scintillators per sector, each 2.5 cm thick, used for triggering and particle identification. The Cerenkov detectors sat behind the wire chambers, containing n=1.02 or 1.03 aerogel for electron/pion discrimination. The neutron detectors were built from 10 cm thick scintillator bars in the left sector (for a neutron detection efficiency of about 10%); the right sector contained either bars of 10 and 20 cm thickness, or two sets of 15 cm bars, for a total thickness of 30 cm (neutron detection efficiency of about 30%). Events were selected using a two-level programmable trigger that produced eight different event types. Data were digitized in FASTBUS ADCs and TDCs and read out with the JLab CODA system.

Over 3 MCoulombs of beam were delivered to the BLAST target in the span of 16 months. Polarized hydrogen data taking consisted of 94 pb^{-1} (see Haiyan Gao's contribution to this conference), while polarized deuterium data taking totalled 420 pb^{-1}. Data were also accumulated on unpolarized hydrogen and deuterium targets for calibration purposes, and on an empty target cell for background measurements.

3 Quasielastic d(e,e′p)

These results are part of the thesis work of Aaron Maschinot of MIT [3]. Events were selected based on particle ID, and a missing mass cut was applied to ensure the events were due to quasielastic scattering. The events were sorted by momentum transfer, and beam and target helicity states. Theoretical calculations were supplied by Arenhövel [2], using the Bonn potential, including meson exchange currents, isobar currents, relativistic corrections, and final state interactions. The theory was implemented in a GEANT Monte Carlo that takes into consideration the BLAST acceptance. At low Q^2, for the lowest missing momentum bins, the theoretical beam-target vector asymmetry is insensitive to the choice of potential, and so the measured A^V_{ed} can be used to extract the product of the beam and target polarizations. Fig. 2 shows the measured asymmetry as a function of missing momentum, for two of the four measured Q^2 bins, for both momentum transfer perpendicular (sensitive to $G^p_E G^p_M$) and parallel (sensitive to G^{p2}_M) to the target vector spin direction. Also shown are the theoretical calculations mentioned above.

At high missing momentum, reaction mechanism contributions are needed in the theory to explain the data. At intermediate momentum transfers it appears that the data rise at a lower missing momentum than the theory, especially in perpendicular kinematics. This trend is still being studied to be sure there is no Q^2-dependent background that has not been accounted for in the data.

Fig. 3 shows the measured tensor asymmetry as a function of missing momentum, for the lowest of four measured Q^2 bins, in perpendicular and parallel kine-

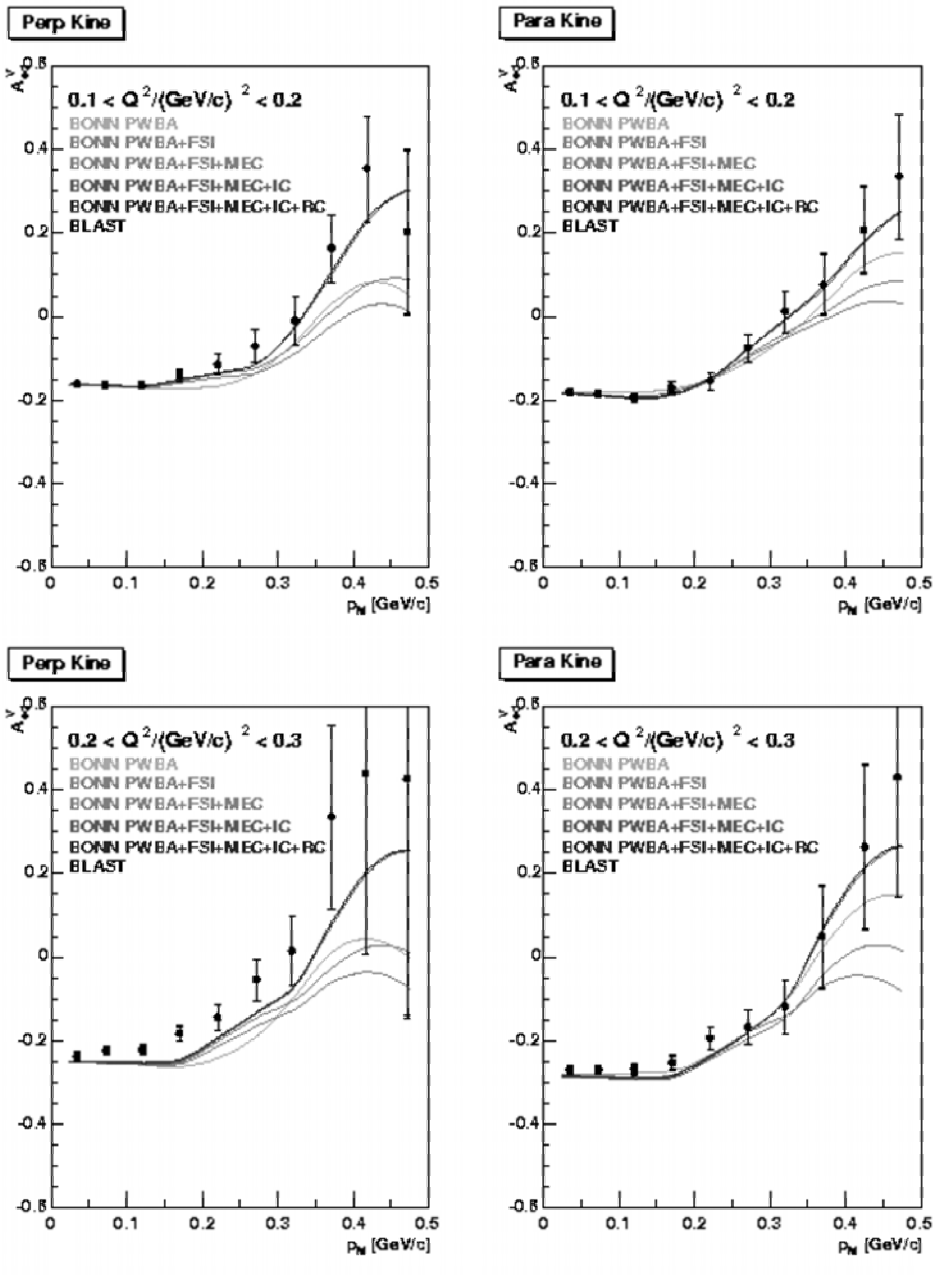

Fig. 2. Preliminary beam target vector asymmetry as a function of missing momentum for Q^2 bins from 0.1 to 0.2 GeV^2/c^2 (top) and 0.2 to 0.3 GeV^2/c^2 (bottom). Perpendicular kinematics are in the left panels, parallel in the right.

matics. Here, P_{zz} has been taken from the elastic scattering measurement, discussed

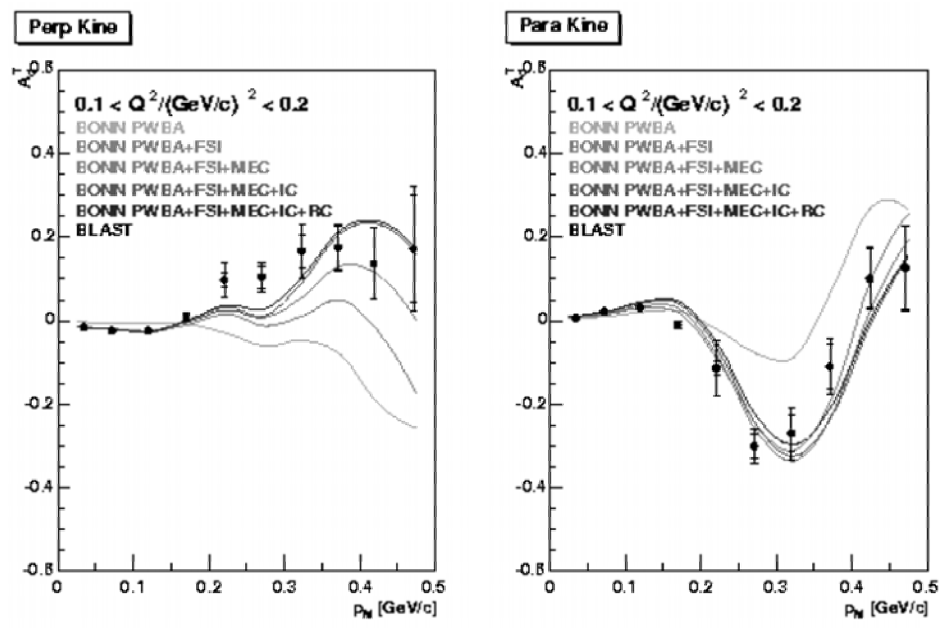

Fig. 3. Preliminary target tensor asymmetry as a function of missing momentum for the lowest Q^2 bin from 0.1 to 0.2 GeV^2/c^2.

further in the fifth section. Again, the full theoretical model is needed to describe the data, not the simple plane wave Born approximation. At low momentum transfer, the measured asymmetry deviates from zero at lower missing momentum than predicted by theory, possibly indicating an earlier onset of D-state structure; this is especially noticeable in parallel kinematics. The data shown here represent about half of the accumulated data; analysis of the remainder is underway.

4 Quasielastic d(e,e′n) and the extraction of G_E^n

These results are part of the thesis work of Vitaliy Ziskin of MIT [4]. Events were selected based on an electron in one sector, and a neutron detector hit in the other sector, with the TOF and wire chambers used as a veto in the neutral particle sector. A cut was placed on the coincidence time difference to eliminate prompt photons. The neutron momentum was extracted from the time of flight measurement. Timing calibrations were performed frequently using both cosmic rays and a laser flasher system. Further cuts were placed on the invariant mass to ensure quasielastic scattering, and missing mass at the mass of the proton.

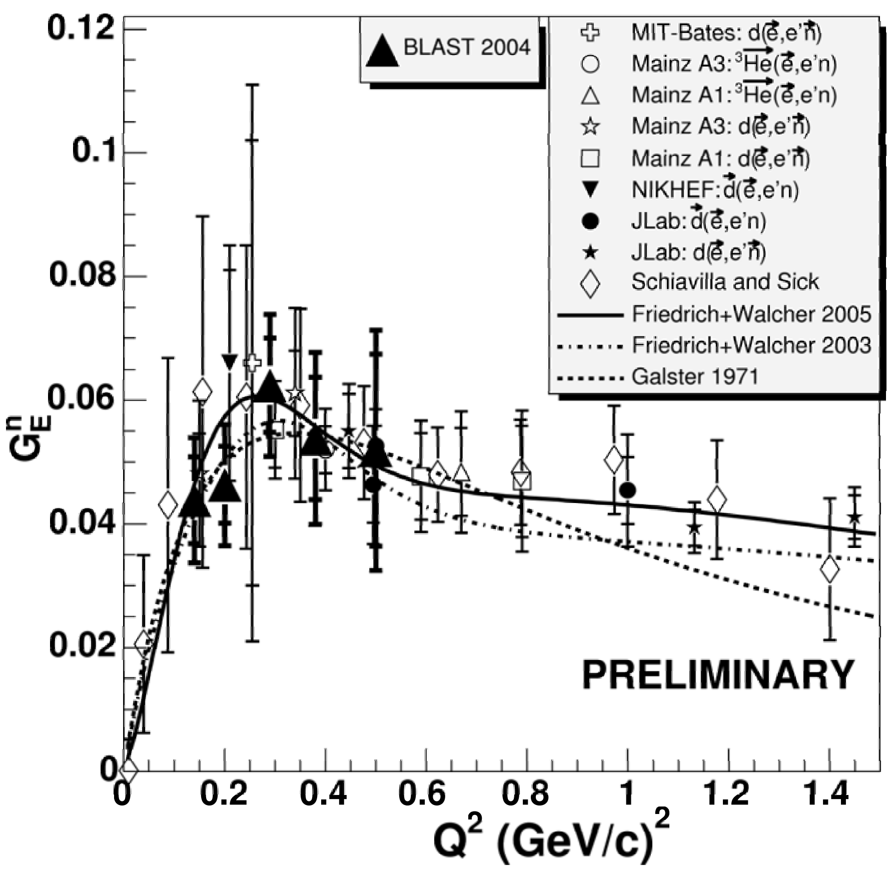

Fig. 4. Electric form factor of the neutron from polarization experiments, including preliminary BLAST results. Random and systematic uncertainties are added in quadrature.

Both hydrogen data and empty target data were used to measure backgrounds. Experimental asymmetries were formed based on the electron and target helicities. To compare with theoretical asymmetries, the measured asymmetry was divided by hP_z measured in d(e,e′p), as detailed in the previous section.

The measured asymmetry at each Q^2 was compared with a Monte Carlo calculation using Arenhövel's theory [2], with the Bonn potential and meson-exchange currents, isobar currents and final state interactions. $G_E^n(Q^2)$ was selected by find-

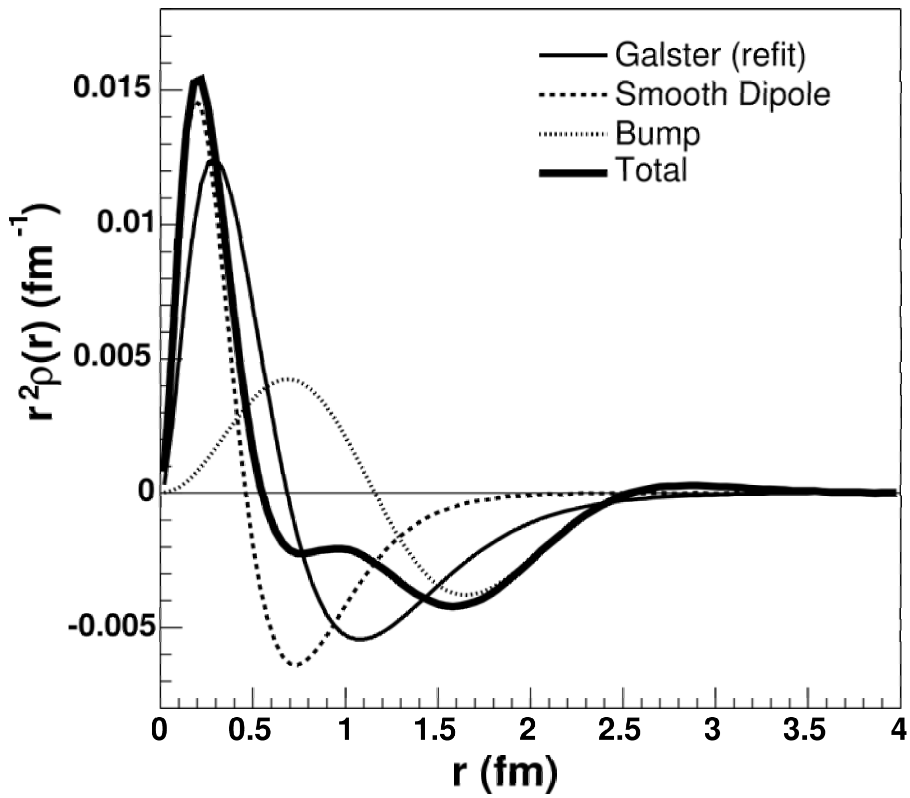

Fig. 5. Fourier transforms of G_E^n parameterizations that include the BLAST data.

ing the value that gave the best fit to the asymmetry as a function of missing momentum. Fig. 4 shows the preliminary BLAST results for about half of the data set, compared with G_E^n extracted from other polarization measurements [6]. The dashed curve is the Galster parameterization [7]. The solid and dash-dot curves are fits using the Friedrich and Walcher parameterization [8], with and without the BLAST data. Although not relativistically correct, a Fourier transform of the form factor gives a sense of the charge distribution of the neutron. Fig. 5 shows the Fourier transform of the FW parameterization that includes the BLAST data. The positive core is due primarily to the dipole term. The bump in G_E^n at low Q^2 gives a negative shell, due to a diffuse pion cloud. Again, the data shown here represent about half of the accumulated data, with analysis of the remainder ongoing.

5 T_{20}

These results are part of the thesis work of Chi Zhang of MIT [5]. The event sample consisted of a scintillator hit in each sector, with wire chamber tracks. A coplanarity cut was applied, as well as a kinematic cut on the scattering angles. Then a cut on the difference in particle arrival times was made, resulting in a clean e-d elastic sample. From this sample, the asymmetry in the target tensor

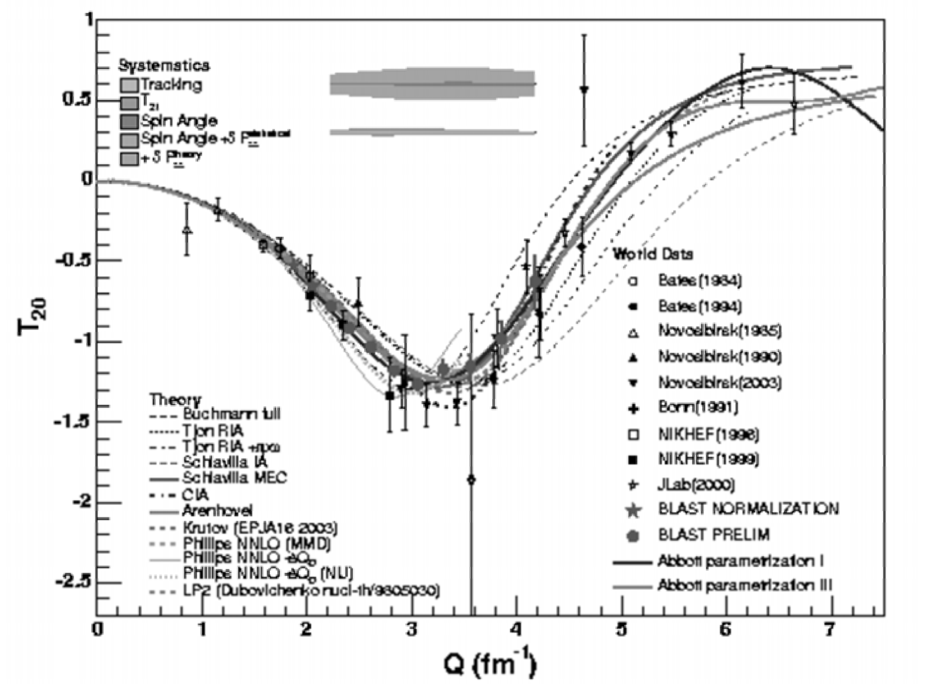

Fig. 6. World data on T_{20}, including the preliminary BLAST results and various theoretical predictions. The systematic uncertainty bands are shown at the top.

polarization was formed. To extract T_{20}, it was necessary to fit the two lowest Q^2 points to a parameterization of the world's data on T_{20} [9], as there was no target polarimeter in this experiment to measure P_{zz}.

Fig. 6 shows the results for T_{20} as a function of Q^2, using a parameterization of the world's data for T_{21}, along with other world data and various theoretical predictions. Shown at the top are the systematic uncertainty bands, dominated by the normalization for P_{zz}. Fig. 7 shows an alternative way to extract both T_{20} and T_{21} from the BLAST data. These points represent the full data set. The BLAST

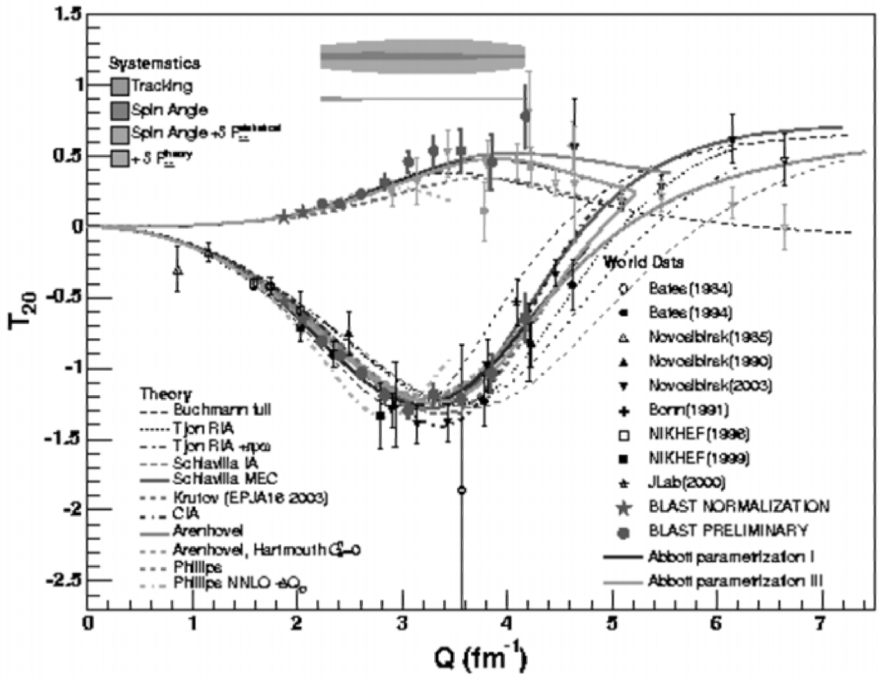

Fig. 7. World data on T_{20} and T_{21}, including the preliminary BLAST results.

data provide an internally consistent and clean set of measurements over a wide range of Q^2, and will help to constrain theoretical models of the deuteron ground state.

6 Conclusion

The BLAST collaboration has taken extensive high quality data on both elastic and inelastic scattering of polarized electrons from a vector and tensor polarized deuterium target. A portion of the deuterium data has been presented here, and more data are being analyzed. The complete data set from the symmetric BLAST detectors, with the use of asymmetry measurement techniques, should provide abundant information on nucleon and deuteron form factors, and help to constrain theoretical models.

This work was supported in part by DOE under Cooperative Agreement DE-FC02-94ER40818

References

[1] H. Arenhövel, W. Leidemann and E.L. Tomusiak: Z. Phys. A **331** (1988) 123.

[2] H. Arenhövel, W. Leidemann and E.L. Tomusiak: Eur. Phys. J. A **23** (2005) 147.

[3] A.J. Maschinot, PhD thesis, Massachusetts Institute of Technology, USA (2005).

[4] V. Ziskin, PhD thesis, Massachusetts Institute of Technology, USA (2005).

[5] C. Zhang, PhD thesis, Massachusetts Institute of Technology, USA (in preparation).

[6] D.I. Glazier et al.: Eur. Phys. J. A **24** (2005) 101, and references therein.

[7] S. Galster et al.: Nucl. Phys. B **32** (1971) 221.

[8] J. Friedrich and Th. Walcher: Eur. Phys. J. A **17** (2003) 607.

[9] D. Abbott et al.: Eur. Phys. J. A **7** (2000) 421.